Science Advances
AAAS

advances.sciencemag.org/cgi/content/full/5/5/eaav4986/DC1

Supplementary Materials for

Photon superbunching from a generic tunnel junction

Christopher C. Leon*, Anna Rosławska, Abhishek Grewal, Olle Gunnarsson, Klaus Kuhnke*, Klaus Kern

*Corresponding author. Email: c.leon@fkf.mpg.de (C.C.L.); k.kuhnke@fkf.mpg.de (K.Ku.)

Published 10 May 2019, *Sci. Adv.* **5**, eaav4986 (2019)
DOI: 10.1126/sciadv.aav4986

This PDF file includes:

Supplementary Text

Calculation of the quantum efficiencies for 1- and 2-photon emission

We present a time dependent calculation of electron tunneling for a one dimensional model, illustrated in Fig. S1. The electrons are assumed to be noninteracting, but they interact with a photon mode in the vacuum region. For time $t < 0$, the tip is assumed to be very far from the substrate, and at $t = 0$ the tip is moved to the position in the figure. For $t > 0$ the Hamiltonian is then given by

$$H = \sum_{n\sigma} \varepsilon_n \, c_{n\sigma}^{\dagger} c_{n\sigma} + \Omega a^{\dagger} a + \sum_{nm\sigma} g_{nm} \, c_{n\sigma}^{\dagger} c_{m\sigma} (a^{\dagger} + a) \qquad \text{(Eq. 1)}$$

where ε_n is the energy of one-particle solutions to the potential in Fig. S1 and $c_{n\sigma}^{\dagger}$ is the corresponding creation operator for an electron with spin σ. Ω is the energy of a photon and $a^{\dagger}$ is its creation operator. The coupling g_{nm} to the photon is calculated by taking matrix elements of the operator $\mathbf{p} \cdot \mathbf{A} + \mathbf{A} \cdot \mathbf{p}$, where $\mathbf{A}$ is the vector potential in the vacuum region and $\mathbf{p}$ is the momentum operator. For simplicity, we only consider one photon state, but allow for zero, single or double occupancy of this boson mode.

To perform a time dependent calculation with well-defined initial conditions, we require that at the beginning of the calculation, the electron is localized well inside the tip (and therefore not interacting with photons) and travelling towards the tip surface. Thus, we consider an electron in a Gaussian wave package at $t = 0$ with a full width of the order of $a/4$ moving towards the tip-vacuum interface starting with its center at $a/2$. The wave function is assumed to take the form

$$|\Psi(t)\rangle = \sum_{n} \left[d_n^{(0)}(t) c_{n\sigma}^{\dagger} + d_n^{(1)}(t) c_{n\sigma}^{\dagger} a^{\dagger} + d_n^{(2)}(t) c_{n\sigma}^{\dagger} a^{\dagger} a^{\dagger} \right] |\text{vacuum}\rangle \qquad \text{(Eq. 2)}$$

describing states with zero, one and two photons and with one electron in addition to the Fermi seas of the tip and the substrate. These Fermi seas are described by $|\text{vacuum}\rangle$. The electron in the wave package is not allowed to fall into the occupied states of the Fermi seas. The width of the wave package, $a/4$, ensures that at $t = 0$, the package is fully inside the metal, so the amplitude at the tip surface is five orders of magnitude smaller than the maximum value inside the tip, so that it justifies the neglect of the interaction with photons at $t = 0$. In other words, $d_n^{(i)}(t = 0) = 0$ for $i = 1$ and 2. The expansion of the wave package in the eigenstates of the potential in Fig. S1 then determines $d_n^{(0)}(t = 0)$.

The time dependent Schrödinger equation is then solved, using the ansatz in Eq. 2. When the wave package reaches the tip-vacuum interface, most of the package is reflected back into the tip, but a small part tunnels through the barrier. In the vacuum region the wave package interacts with photons, and we allow for the possibility of the emission of one or two photons. When the tunneling part of the wave package is well past the vacuum region, we integrate the parts with zero, one or two photons over the substrate region, obtaining the weights w_0, w_1 and w_2, respectively. The quantum efficiencies are then $k_1 = w_1/w_0$ and $k_2 = w_2/w_0$.

We first perform calculations only including electronic states at lower energies than the original wave package, assuming that the electron can only lose energy due to photon emission. We then typically find that k_2 is about three orders of magnitude smaller than k_1^2. For instance, with a_0 being the Bohr radius, we use the parameters $a = c = 6400\, a_0$, $b = 15\, a_0$, $\varepsilon_F = 8$ eV, $\Phi = 4.5$ eV, $\Omega = 2$ eV and $V = 5$ eV. These particular values of *a*, *c*, and *b* are chosen based on the following considerations. The value of *a* determines the spread in wave vector space of the wave package, and is chosen to be large enough so that the momentum spread, proportional to 1/*a*, is very small (about 0.4 per cent, which is less than a percent of the Fermi wave vector) and the electron has a rather well defined *k*-vector. The value *c* is chosen to be large enough to ensure that at the end of the calculation, the wave package that tunnels through the barrier has moved so far from the barrier that it is fully contained in the metal and the interaction with photons can again be neglected. This makes it possible to measure the number of emitted photons and the electron energy in a well-defined way. The value of $b = 15\, a_0 \sim 0.8$ nm is chosen to be a typical tip-surface distance.

For these parameters we find that $k_2/k_1^2 = 0.001$. In a one photon emission event, the electron falls from ε_F to $\varepsilon_F - \Omega$. The initial state decays exponentially in (most of) the vacuum region; the final state having lower energy, decays even more strongly. The corresponding matrix element g_{nm} is then small. For a two photon event this effect is even stronger. In the first photon emission event the electron falls to a lower state (not necessarily to $\varepsilon_F - \Omega$) and in the second event it falls to $\varepsilon_F - 2\Omega$. The second transition then involves states that are more strongly exponentially decaying than for the first transition and the corresponding matrix element g_{nm} is much smaller. This leads to $k_2 \ll k_1^2$ in this calculation. Combined with the experimental observation that k_2 can be more than two orders of magnitude larger than k_1^2, this then makes k_2 about five orders of magnitude larger than might have been expected.

It is interesting, however, that if we include electronic states higher than the initial state (extending up to, *e.g.*, 70 eV), we obtain $k_2/k_1^2 = 0.4$ for the parameters above, almost three orders of magnitude larger than above. In the dominating two-photon process the electron is now excited *upwards* in energy, getting close to the top or even above the barrier in the first photon emission event. The electron can then propagate (more) freely through the vacuum. In the second photon emission event it then falls down into a state low enough that the energy of the overall process is conserved. This leads to a large enhancement of the two photon process for two reasons; (i) in both transitions one of the two wave functions entering the matrix elements is not exponentially decaying (over most of the vacuum region) and (ii) the electron excited above (or close to the top of) the barrier can more easily propagate through the vacuum region.

Although this new mechanism greatly enhances two-photon events, the corresponding k_2/k_1^2 is still much smaller than seen experimentally. This could possibly be due to the model being too simple, but a more likely explanation may be that this is not the leading mechanism for two-photon events, raising interesting questions.

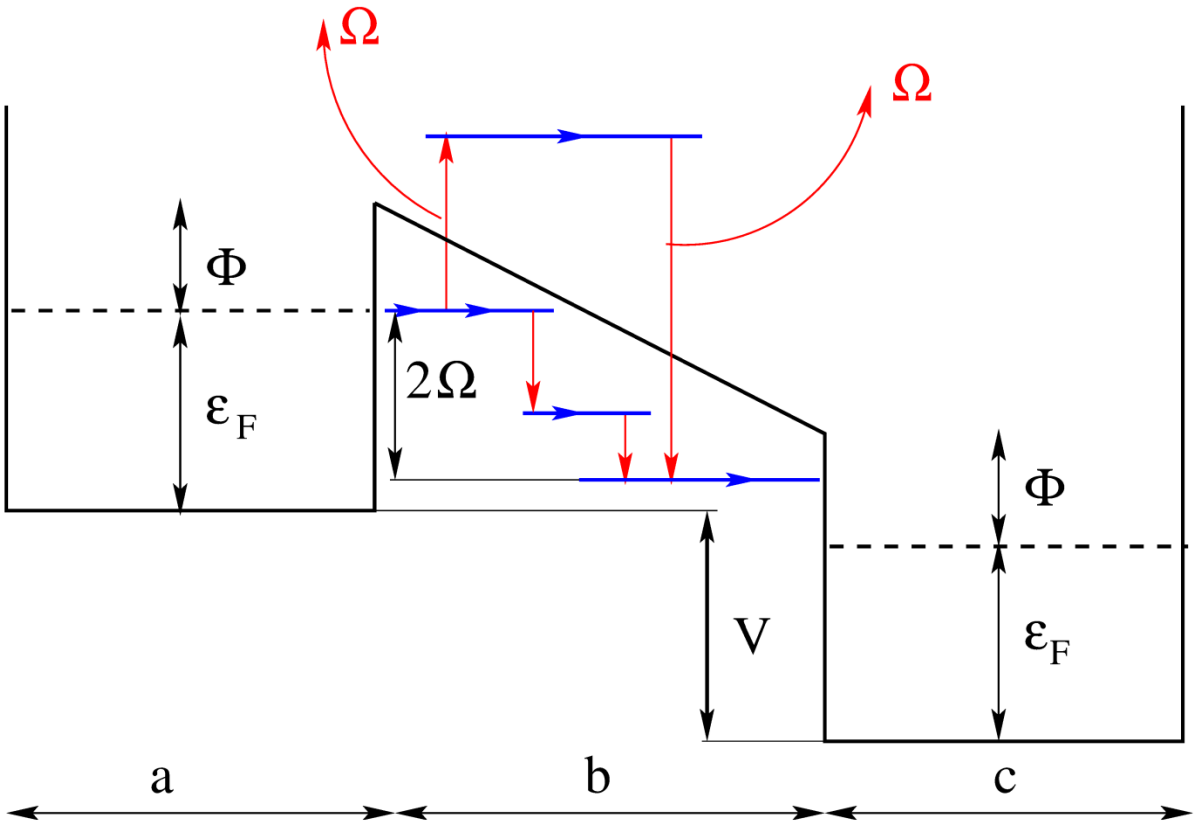

Fig. S1. Schematic of a one-dimensional model of tunneling. The tunneling begins from the tip (left), described by a potential well of width a, through vacuum region of width b to a substrate of width c (right). The Fermi energy is ε_F, the work function Φ, the voltage across the barrier V, and the photon energy Ω. Blue lines indicate energies of electronic levels in the vacuum region, blue arrows represent propagation of an electron with a certain energy through the vacuum region and red arrows represent two different types of two-photon emission events together with electronic transitions.

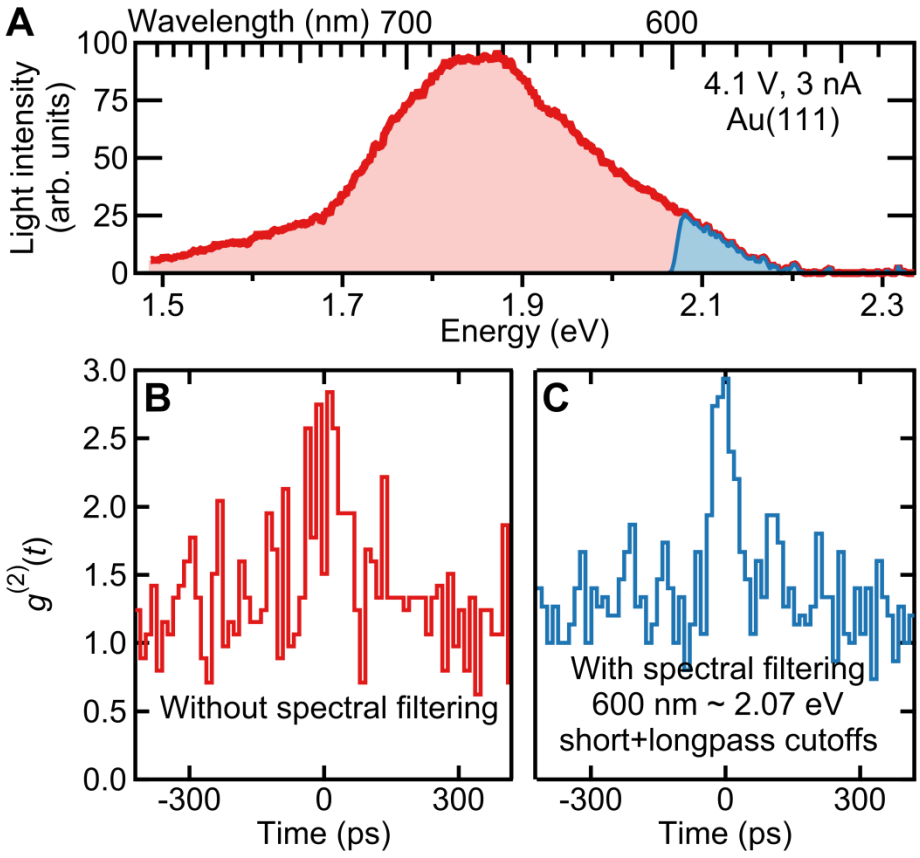

Fig. S2. Photon correlation measurements at fixed tunnel conditions with varied spectral filtering for a gold tip on Au(111). (**A**) Measured optical spectrum (red) and its shortpass 600 nm cutoff spectrum (blue); longpass 600 nm cutoff not shown. (**B**) Bunching is observed in the unfiltered light, just as in Figure 5B. (**C**) Bunching is also observed when high and low energy photons enter separate detectors (F1 = shortpass filter, F2 = longpass filter in Figure 1). Total data accumulation time in seconds: (**B**) 600, (**C**) 34000. Accidental correlation level in events per bin: (**B**) 11.27, (**C**) 14.98.

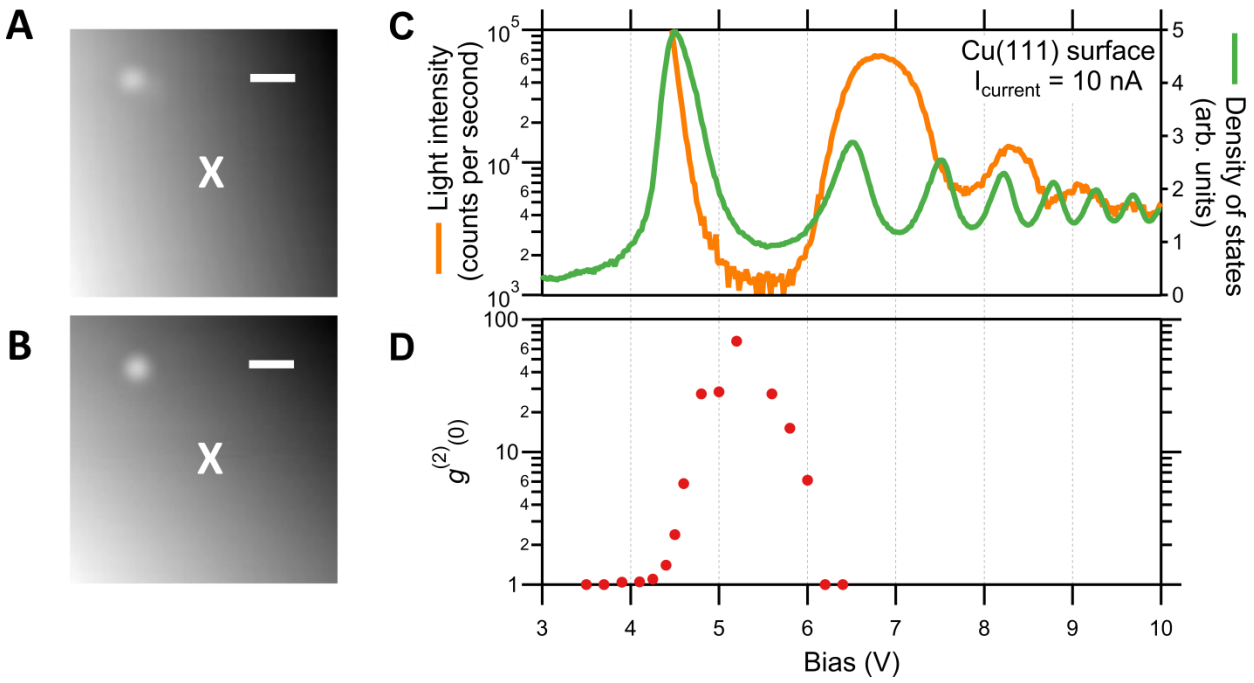

Fig. S3. Survey measurements of bunching for a gold tip on Cu(111). Surface topography at (**A**) the start, and (**B**) the end of bunching measurements; +3 V, 100 pA, scale bar 1 nm, 6 hour time interval between scans, X marks the position of all spectroscopy and correlation measurements. (**C**) Light intensity and density of states as a function of bias. (**D**) Bunching degree as a function of bias. The range of observable bunching (~3–6 V) coincides with twice the photon counter sensitivity range (~1.5–3 V), and hence, is consistent with a $1e^- \rightarrow 2\gamma$ process.